

Phase Transitions in the Anchored Organic Bilayers of Long-Chain Alkylammonium Lead Iodides $(C_nH_{2n+1}NH_3)_2PbI_4$; $n = 12, 16, 18$

S. Barman,[†] N. V. Venkataraman,[‡] S. Vasudevan,^{*,†,‡} and Ram Seshadri^{*,†,§}

Solid State and Structural Chemistry Unit and Department of Inorganic and Physical Chemistry, Indian Institute of Science, Bangalore-560012, India

Received: August 30, 2002; In Final Form: December 4, 2002

The single perovskite slab alkylammonium lead iodides $(C_nH_{2n+1}NH_3)_2PbI_4$, $n = 12, 16, 18$, display two phase transitions, just above room temperature, associated with changes in the alkylammonium chains. We have followed these two phase transitions using scanning calorimetry, X-ray powder diffraction, and IR and Raman spectroscopies. We find the first phase transition to be associated with symmetry changes arising from a dynamic rotational disordering of the ammonium headgroup of the chain whereas the second transition, the melting of the chains in two dimensions, is characterized by an increased conformational disorder of the methylene units of the alkyl chains. We examine these phase transitions in light of the interesting optical properties of these materials, as well as the relevance of these systems as models for phase transitions in lipid bilayers.

Introduction

Alkylammonium lead iodides with the general formula $(C_nH_{2n+1}NH_3)_2PbI_4$ comprise perovskite-like PbI_4^{2-} slabs that are flanked on either side by cationic alkylammonium chains $C_nH_{2n+1}NH_3^+$.¹ These are important materials because their intrinsic organic (insulating)–inorganic (semiconducting) structures are akin to “natural quantum-well” architectures.^{2–5} Associated with these quantum-well structures are tunable excitonic properties that depend crucially on the dielectric properties, governed usually by the chain length of the insulating organic layer.^{5,6}

An understanding of phase transitions in the organic part of these hybrid structures is therefore quite important from the materials viewpoint. In addition, because bilayer lipids are ubiquitous in the natural world, it is of great interest to study phase transitions in model systems that share similarities with lipid bilayers. Phospholipid bilayers are known to undergo structural phase transitions with temperature.⁷ The widely studied dipalmitoylphosphatidicholine (DPPC), for example, exhibits two endothermic transitions,⁸ a premelting transition at 308 K and a main transition at 313 K. The nature of the premelting transition is poorly understood; reorientation and a change in the tilt of the acyl chains has been suggested.^{9,10} The main transition is associated with the melting of the acyl chains⁷ leading to increased conformational disorder of the chains. Unlike free lipid bilayers, the title compounds have one end anchored to an inorganic lattice that is quite rigid. In the temperature range of interest, the inorganic lattice undergoes no change. Heat provided to the system can result in changes in chain conformation and orientation but cannot vastly modify interchain distances. Many inorganic–organic hybrid systems based on the layered perovskite structure containing long ($n >$

12) alkylammonium chains are known to exhibit one or more phase transitions with temperature.^{11–17} Most studies have concluded that the main transition appearing at higher temperatures is a melting of the alkyl chains—a behavior similar to that in lipid bilayers.⁷ On the basis of NMR measurements on $(C_{10}H_{21}NH_3)_2CdCl_4$, it has been suggested that the low-temperature transition, exhibited by some these compounds, is a dynamic disordering of the rigid alkyl moieties.¹³

In this study, we present a detailed examination of phase transitions associated with the organic moieties in the layered alkylammonium lead iodides $(C_nH_{2n+1}NH_3)_2PbI_4$, $n = 12, 16, 18$. The techniques used include differential scanning calorimetry (DSC), powder X-ray diffraction (XRD), FT-IR spectroscopy, and Raman spectroscopy. The XRD and spectroscopic studies have been carried out as a function of temperature. This combination of techniques has allowed us to examine in detail the precise nature of the phase transitions—to relate changes in the crystal lattice with changes in the conformation of the alkylammonium chains. In addition, the variation of the alkylammonium chain length n has allowed us to follow systematically the influence of the number of methylene units in the organic moiety on the phase transition.

Experimental Section

The title compounds were prepared by mixing stoichiometric quantities of PbI_2 and $C_nH_{2n+1}NH_2$ in hydroiodic acid (57%) and refluxing to obtain a clear yellow solution. The solution was slowly cooled to precipitate the $(C_nH_{2n+1}NH_3)_2PbI_4$ compounds,¹⁸ which were obtained as flakes a few millimeters on edge. The compounds were washed with water till the filtrate showed a complete absence of acid.

The thermal behavior of the compounds was investigated by differential scanning calorimetry using a Perkin-Elmer DSC 2C instrument operated at a scanning rate of 5 K min^{−1} under an N₂ atmosphere. The temperature scale and the enthalpy were calibrated using an indium standard ($T_m = 429$ K, $\Delta H_m = 28.5$ J g^{−1}). Powder X-ray diffraction patterns as a function of temperature were acquired on a Shimadzu XD-D1 diffractometer

* Corresponding authors. E-mail: S.V., svipc@ipc.iisc.ernet.in; R.S., seshadri@mrl.ucsb.edu.

[†] Solid State and Structural Chemistry Unit.

[‡] Department of Inorganic and Physical Chemistry.

[§] Present address: Materials Department, University of California, Santa Barbara, CA 93106-5050.

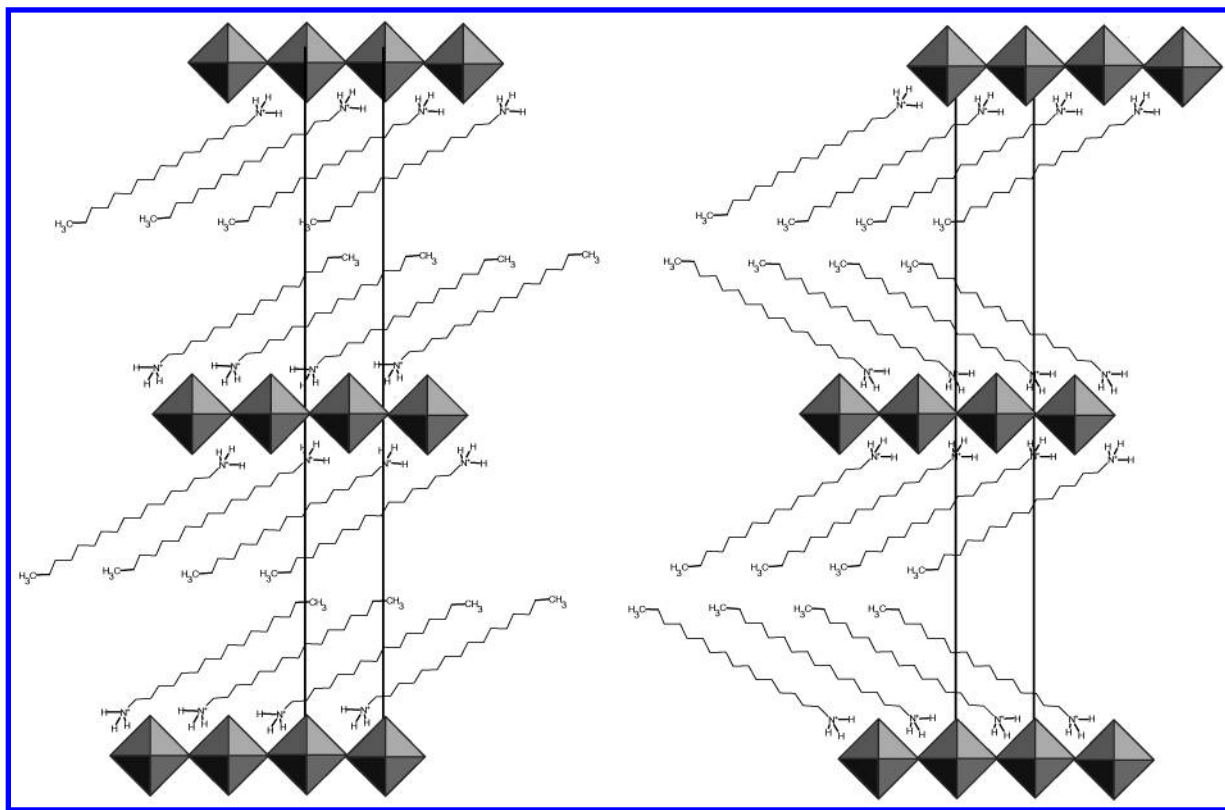


Figure 1. Schematic depicting the two possible structures of the alkyl chains in the layered $(C_nH_{2n+1}NH_3)_2PbI_4$ compounds.

operated in the θ - 2θ Bragg-Brentano geometry. The samples were mounted on an aluminum block that could be heated in a controlled manner. FT-IR spectra of the title compounds were recorded as KBr pellets on a Bruker IFS55 spectrometer operating at 4 cm^{-1} resolution. FT-Raman spectra were recorded on a Bruker IFS FT-Raman spectrometer using an Nd:YAG ($\lambda = 1064\text{ nm}$) laser for excitation. Spectra were recorded at a resolution of 4 cm^{-1} . For both IR and Raman studies, the sample holders were modified such that heating in a controlled manner was possible.

Results and Discussion

In two earlier papers,^{18,19} we have used a number of techniques including X-ray diffraction and vibrational and ^{13}C NMR spectroscopy to arrive at a consistent picture of the room-temperature structure of the three compounds, $(C_nH_{2n+1}NH_3)_2PbI_4$, $n = 12, 16, 18$. Figure 1 shows schematics of the structure for the $n = 16$ compound. The salient features of these long chain alkylammonium lead iodides follow: (i) The inorganic portions of the structure remain invariant as the number of carbon atoms in the alkylammonium chains is changed. This is verified from the 1-D projections of the electron densities obtained from a Fourier transforms of the $00l$ reflections in the XRD patterns.¹⁸ (ii) The alkylammonium chains are all-trans at room temperature.¹⁹ (iii) The chains are not interdigitated but, rather, are possessed of a fixed tilt angle that is 55° from the normal to the layers.¹⁸ Our studies do not allow us to distinguish between one of two possible structures displayed in Figure 1, the one a structure where the bilayers are opposed and the other a structure where the bilayers form a herringbone pattern.

In the rest of this section, we report the temperature dependence of the structure, with a focus on what happens to the conformation and disposition of the organic moieties as the temperature is raised.

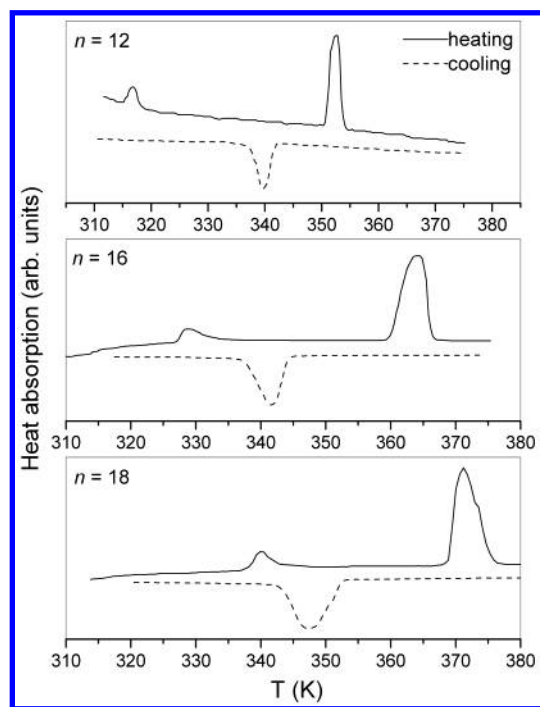


Figure 2. Heating (solid line) and cooling (dashed line) DSC runs of the layered $(C_nH_{2n+1}NH_3)_2PbI_4$ compounds of different chain lengths: (a) $n = 12$, (b) $n = 16$, and (c) $n = 18$.

Thermal Studies. Figure 2 displays differential scanning calorimetric traces for the three compounds $(C_nH_{2n+1}NH_3)_2PbI_4$, $n = 12, 16, 18$. On heating, we observe two endotherms corresponding to first-order phase transitions. Cooling results in one exotherm, corresponding to the second transition of the heating run. Consistent with the lipid literature, we refer to the two transitions on heating as the premelting and the melting transitions.⁷ The premelting transition is not seen when the

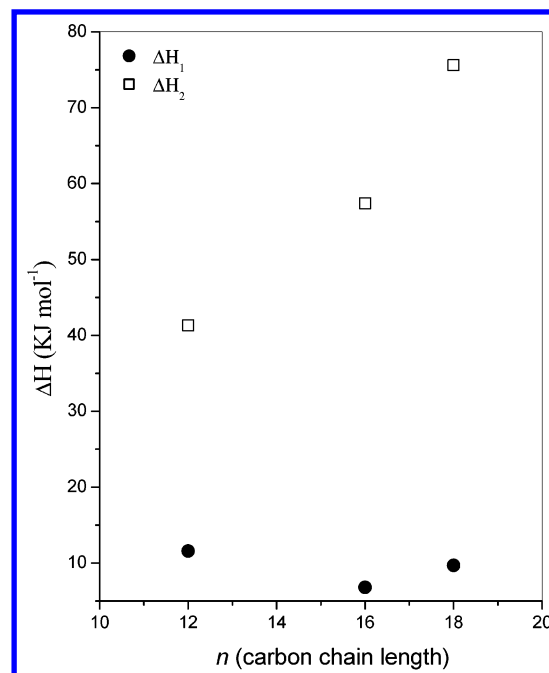
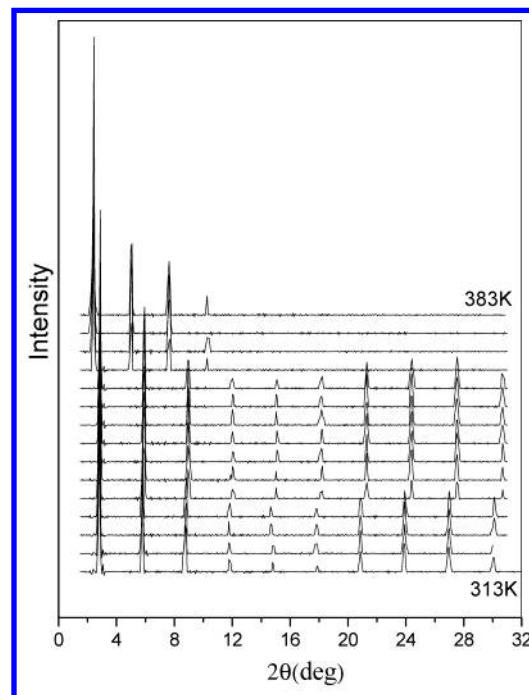
TABLE 1: Summary of the Transition Enthalpies and Entropies Accompanying the Premelting (T_1) and Melting (T_M) Transitions in $(C_nH_{2n+1}NH_3)_2PbI_4$ Compounds of Different Chain Lengths

chain length (n)	T_1 (K)	ΔH_1 (kJ mol $^{-1}$)	T_M (K)	ΔH_2 (kJ mol $^{-1}$)	ΔS_2 (J K $^{-1}$ mol $^{-1}$) (per CH $_2$ unit)
12	318	11.6	353	41.3	10.7
16	331	6.8	364	57.4	10.6
18	341	9.7	373	75.6	11.9

sample is heated again, but on keeping the samples for some days and repeating the calorimetric study, both transitions are recovered in the heating run. We observe that both the premelting and the melting transition temperatures increase with increasing carbon chain length n in these compounds (Table 1). When we plot the heats of these transitions as a function of chain length (Figure 3), we observe that the heat of the premelting transition is small (of the order of 10 kJ mol $^{-1}$) and somewhat independent of the length n of the carbon chain. The heat of the second transition scales with the carbon chain length. We find, however, that at the melting transition, the entropy change per CH $_2$ in the chain is nearly constant across the three compounds and is equal to about 11 J K $^{-1}$ mol $^{-1}$ (Table 1). The second, melting transition therefore displays certain universal features. Table 1 summarizes the temperatures and the heats of the two transitions for the three compounds. The ΔH values for the melting transition are comparable with values reported for similar inorganic–organic layered systems.¹⁵

Powder X-ray Diffraction. Figure 4 displays the temperature dependence of the powder X-ray diffraction pattern for a typical compound $(C_nH_{2n+1}NH_3)_2PbI_4$ ($n = 16$). Because of the highly lamellar nature of these compounds, the XRD patterns reveal only 00 l reflections, which were indexed⁵ as 002, 004, 006, The data were recorded from a temperature of 303 to 383 K at intervals of 5 K. It is seen that at the temperature corresponding to the premelting transition, T_1 , the peaks are shifted to a higher Bragg angle, corresponding to a shrinking of the inter-inorganic slab distance. After the second, melting transition, the peaks are shifted back toward the lower Bragg angle, corresponding to lattice expansion along the c -axis-increased inter-inorganic slab spacing. The change in the c parameter (taken as twice the inter-inorganic slab spacing) as a function of temperature is displayed for all three compounds (both heating and cooling runs) in the three panels of Figure 5. The lines, which are guides to the eye, show clearly that the premelting transition corresponds to a small contraction in the c parameter, whereas the melting transition corresponds to a large expansion in the c parameter. In keeping with the strongly first-order nature of the transitions, there is significant thermal hysteresis in the transitions. In addition, the room temperature structure is not precisely recovered in the cooling run. It is, however, recovered on keeping the sample for some days; a behavior similar to that observed in the DSC measurements. The observed increase in the interlayer spacing on melting in the $(C_nH_{2n+1}NH_3)_2PbI_4$ compounds may be contrasted with the behavior of lipid bilayers at the gel–liquid crystalline melting transition. In most lipid bilayer systems this transition is accompanied by an increase in volume but with a decrease in the layer thickness.²⁰ The increase in volume being due to a lateral expansion of the bilayers. In the present system, however, the alkylammonium chains are grafted onto the rigid inorganic PbI_4 sheets and no lateral expansion is possible; consequently, the increase in volume on melting is reflected in an increase in the interlayer spacing.

Vibrational Spectroscopic Studies. The “action”, as it were, accompanying the premelting and melting transitions is associ-

**Figure 3.** Variation of transition enthalpies of the premelting, ΔH_1 (closed circles), and the melting transitions, ΔH_2 (open squares), as a function of chain length (n) in the layered $(C_nH_{2n+1}NH_3)_2PbI_4$ compounds.**Figure 4.** Powder X-ray diffraction patterns showing the 00 l reflections in the $(C_{16}H_{33}NH_3)_2PbI_4$ compound recorded at different temperatures across the premelting and melting transitions. The patterns were recorded at every 5 K intervals.

ated with the long hydrocarbon chains in the alkylammonium moieties. Vibrational spectroscopies provide a powerful and quantitative *local* probe of the structure and dynamics in the alkylammonium chains.^{16,17} In this subsection, we describe the temperature-dependent infrared and Raman spectra of the three alkylammonium lead iodides. The temperature variation of the spectral features have been plotted as a function of reduced temperature, T/T_m , where T_m is the temperature at which the second, the melting, transition takes place. This has been done to highlight the universal nature of this transition.

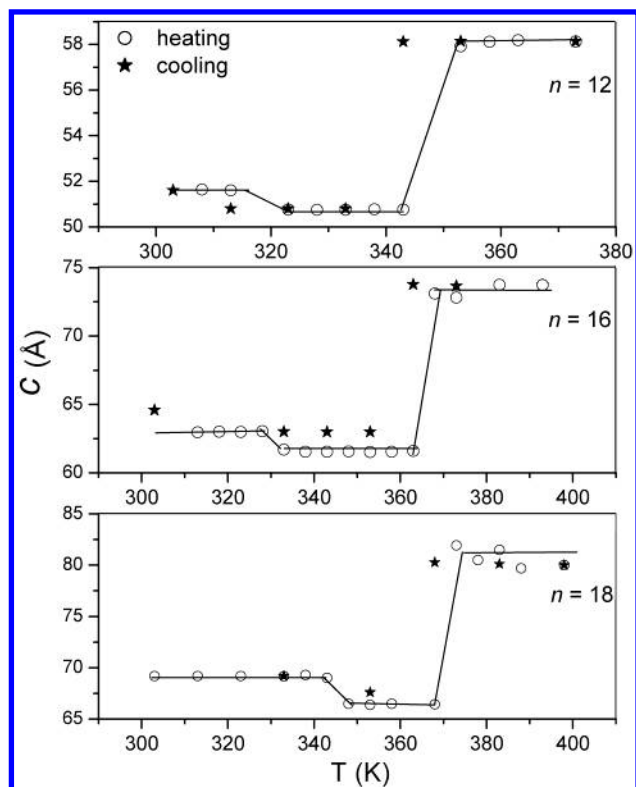


Figure 5. Variation of the interlayer c parameter in $(C_nH_{2n+1}NH_3)_2PbI_4$, $n = 12, 16, 18$ compounds as a function of temperature: (○) heating; (★) cooling. A small decrease in the interlayer spacing may be seen at the premelting transition followed by an expansion at the melting transition.

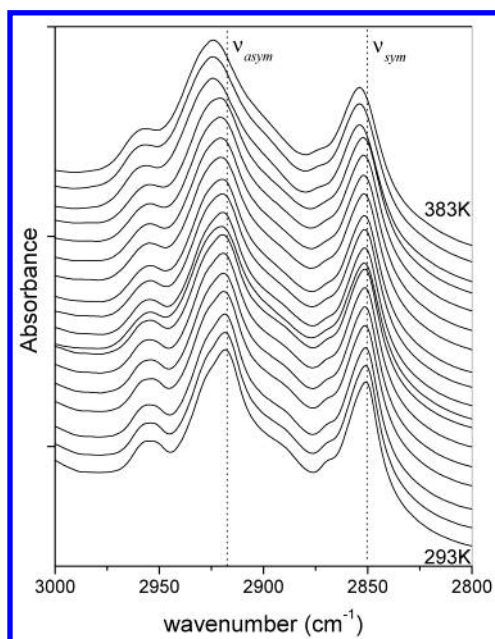


Figure 6. Infrared spectra in the C–H stretching region of the $(C_{16}H_{33}-NH_3)_2PbI_4$ compound recorded at different temperatures between 293 and 393 K. The spectra were recorded at 5 K intervals.

Figure 6 displays the C–H stretching region of the infrared spectrum of the $n = 16$ member of the $(C_nH_{2n+1}NH_3)_2PbI_4$ compounds, recorded at different temperatures, spanning the two phase transitions. In the region displayed, one observes the symmetric and antisymmetric C–H stretches of the methylene groups of the alkylammonium chain, and the symmetric and asymmetric C–H stretches of the terminal $-CH_3$ groups, which are weaker in intensity and appear at 2867 and 2952 cm^{-1} ,

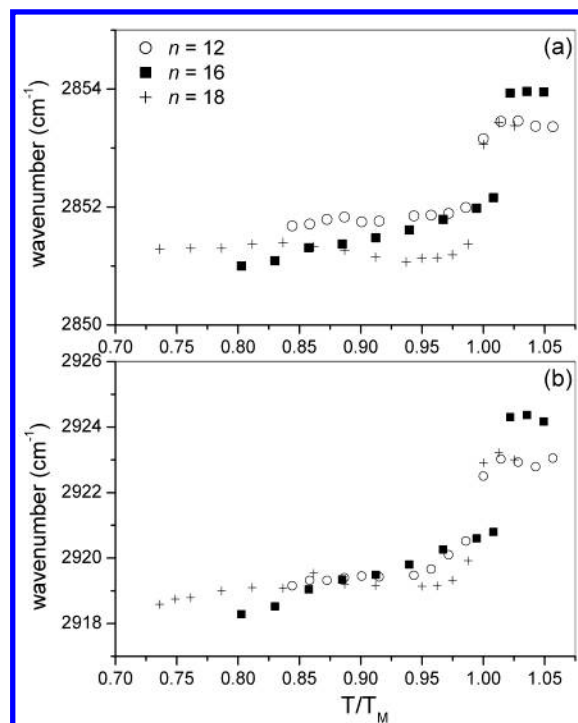


Figure 7. Frequencies of the methylene (a) symmetric and (b) antisymmetric stretching modes in $(C_nH_{2n+1}NH_3)_2PbI_4$, $n = 12, 16, 18$, compounds as a function of reduced temperature T/T_M . T_M is the melting transition temperature.

respectively. Although the latter show no dependence on chain conformation, the positions of the former are sensitive to the chain conformation, shifting to higher frequencies in the presence of gauche disorder.^{21,22} For an all-trans conformation typical values for the methylene symmetric (ν_{sym}) and antisymmetric (ν_{asy}) stretching modes are in the range 2846–2848 and 2916–2918 cm^{-1} , respectively.²¹ With increasing gauche disorder, they shift to higher wavenumbers, typically to 2854–2856 cm^{-1} for ν_{sym} and 2924–2928 cm^{-1} for ν_{asy} .²²

We observe an abrupt shift of the C–H stretch frequencies, both ν_{sym} and ν_{asy} , to higher wavenumbers at the temperature corresponding to the melting transition. We quantify this by plotting (Figure 7) the frequencies of ν_{sym} (panel a) and ν_{asy} (panel b) stretching modes of the $-(CH_2)-$ groups in the chain for the three compounds, as a function of the reduced temperature T/T_m . For all three compounds, it is seen that melting ($T/T_m = 1$) is accompanied by a jump in the C–H stretching frequencies. After the transition, the symmetric C–H stretch ν_{sym} appears at 2854 cm^{-1} whereas ν_{asy} is at 2924 cm^{-1} . These are typical values for hydrocarbon chains with a large number of gauche defects as in alkane melts. It may also be seen that the first, or premelting, transition is not associated with any significant shift in the methylene stretching frequencies.

The methylene scissoring mode at 1467 cm^{-1} and the rocking mode at 720 cm^{-1} are diagnostic of packing arrangements in alkyl chain assemblies.²³ These modes are known to split (correlation splitting) due to interchain interactions into two components in closely packed alkyl chain systems where more than one chain is present per unit cell.²³ In many lipid bilayer systems these bands appear as doublets in the “crystalline” phase, which collapse to a single peak on melting, signifying a change in lateral arrangement.²⁴ For the $(C_nH_{2n+1}NH_3)_2PbI_4$, $n = 12, 16, 18$, the methylene scissoring mode (1467 cm^{-1}) and the rocking mode (720 cm^{-1}) appear as a single peak at all temperatures, indicating that there is no change in the lateral

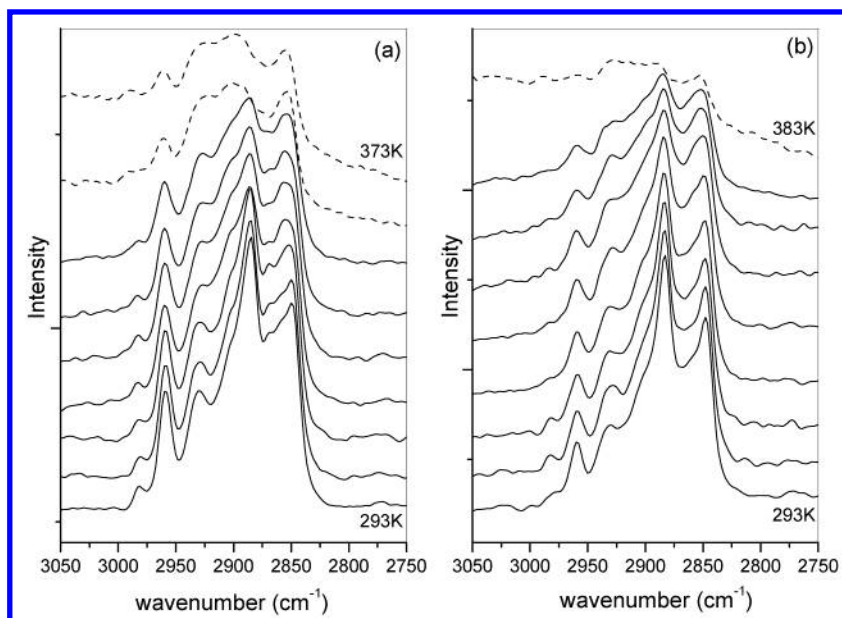


Figure 8. FT-Raman spectra of $(C_nH_{2n+1}NH_3)_2PbI_4$ compounds, (a) $n = 12$ and (b) $n = 16$, recorded at different temperatures. The spectra were recorded at 10 K intervals.

packing arrangement of the alkyl chains. This is not surprising because the alkyl chains are anchored to the PbI_4^{2-} sheets.

Raman spectroscopy in the C–H stretch region has been extensively used to characterize alkyl chain conformation.²⁵ In Figure 8, we display the C–H stretch region of the FT-Raman spectra for the $n = 12$ and $n = 16$ compounds recorded at different temperatures. The assignments of the bands in the room-temperature spectra are similar to that of the alkanes.²⁶ The intense low-frequency band at 2850 cm^{-1} is identified with the symmetric (d^+) C–H stretch fundamental of the methylene group whereas the band at 2890 cm^{-1} is identified with the antisymmetric (d^-) fundamental. The band at 2930 cm^{-1} is assigned to the Fermi resonance of the d^+ mode with the overtone of the bending mode whereas the band at 2960 cm^{-1} is assigned to the in-plane asymmetric stretching (r^-) mode of the methyl group (the assignment and notation is based on that of the crystalline n -alkanes²⁶). From room temperature to just below T_m neither the positions nor line widths of these bands show any significant change; there is, however, a change in the relative intensities of the methylene symmetric and antisymmetric stretching modes. At T_m the spectra change fairly dramatically (the spectra above T_m are shown in dashed lines in Figure 8). At T_m the d^- mode collapses into a featureless broad scattering with its maxima shifted to higher frequencies (2990 cm^{-1}). The position of the methylene symmetric stretching mode, however, shows no change and is the strongest feature of the spectra above T_m .

The spectra of $(C_nH_{2n+1}NH_3)_2PbI_4$ above T_m are typical of the spectra of the alkanes and lipid bilayers above their melting transition. In these systems, too, melting is characterized by the collapse of the antisymmetric d^- mode into a broad band, with the symmetric d^+ mode remaining essentially unchanged.²⁷ It has been suggested that the broadening of the antisymmetric d^- is a consequence of the convolution of bands associated with d^- modes of different quasi-gauche conformers present in the molten state.²⁸ An alternate explanation ascribes the broadening as arising from collective chain flexibility–libration–twist or libration–torsion modes in the melt.²⁹ In the present compound the former explanation for the broadening appears more likely because the infrared spectra had clearly indicated an increase in the concentration of gauche conformers at T_m .

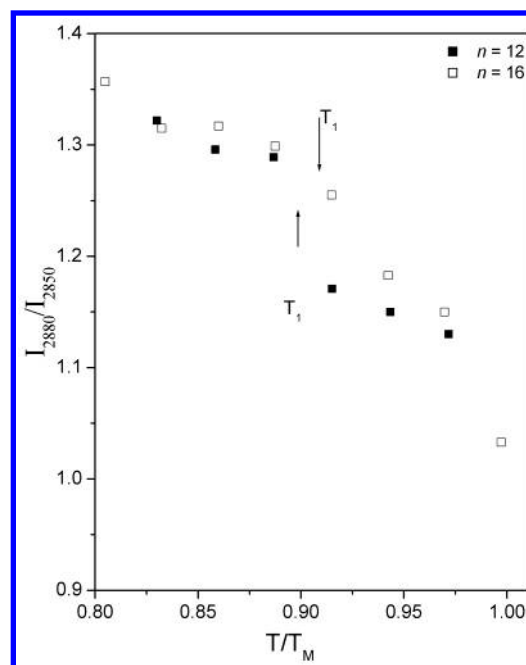


Figure 9. Ratio of the intensities of the methylene antisymmetric and symmetric stretching modes (I_{2880}/I_{2850}) in $(C_nH_{2n+1}NH_3)_2PbI_4$ compounds for two different chain lengths, $n = 12$ and $n = 16$, as a function of reduced temperature (T/T_M). The temperature of the premelting transition is indicated.

It is well-known that the ratio of the intensities of the antisymmetric C–H stretching mode at 2880 cm^{-1} and the symmetric mode at 2850 cm^{-1} (I_{2880}/I_{2850}) is characteristic of conformational disorder as well as packing in alkyl chain assemblies.^{25,26} In crystalline hydrocarbons, the ratio is near 2 and in hydrocarbon melts, it is near 0.7.²⁶ The variation in the ratio, I_{2880}/I_{2850} , as a function of the reduced temperature T/T_m for the $n = 12$ and $n = 16$ compounds is shown in Figure 9 (the ratios are not defined for $T > T_m$ because of the broadening and shift of the antisymmetric mode). In the present system, because no change in the lateral packing arrangement with temperature is possible, the change in the I_{2880}/I_{2850} ratio would be wholly due to changes in alkyl chain conformation. The ratio

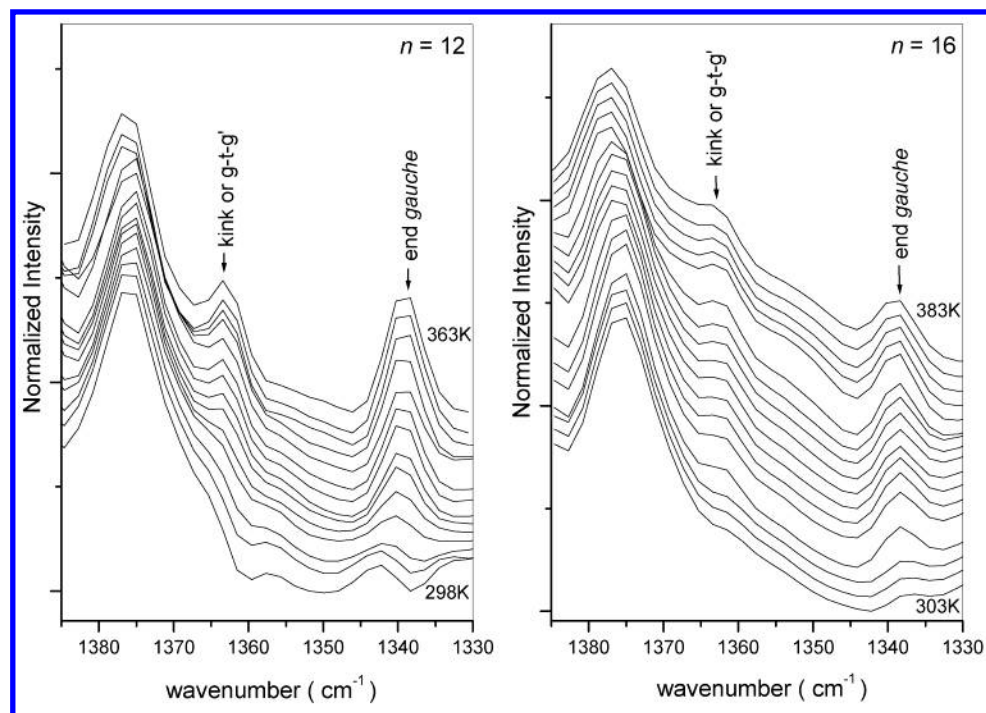


Figure 10. Infrared spectra in the methylene wagging region recorded at different temperatures for the $n = 12$ and $n = 16$ $(C_nH_{2n+1}NH_3)_2PbI_4$ compounds, showing the increase in the intensity of peaks corresponding to “kink” (1366 cm^{-1}) and end-gauche (1341 cm^{-1}) conformations at higher temperatures. The spectra are normalized with respect to the 1377 cm^{-1} CH_3 symmetric bending mode. The spectra were recorded every 5 K interval.

shows a sharp drop at the premelting transition and a steady decrease with temperature above T_1 . Figure 9 indicates that the thermal evolution of conformation disorder is initiated well below T_m .

The methylene stretching modes in the infrared and Raman indicate an increase in gauche conformers with temperature. It is possible to identify specific conformational sequences containing a gauche bond from their characteristic signature in the methylene wagging region of the infrared spectrum.³⁰ Thus a peak at 1341 cm^{-1} indicates a penultimate bond oriented such that the methyl group is in gauche conformation relative to the methylene group three carbons away. A peak at 1354 cm^{-1} is characteristic of two adjacent gauche bonds (double gauche) and a band at 1364 cm^{-1} arises from a kink (successive gauche–trans–gauche conformers in the chain). Because these are localized modes, the area under the peak is proportional to the concentration of the specific bond sequences.³¹ The methyl umbrella deformation mode that appears at 1375 cm^{-1} is taken as an internal standard for normalization because its position is unaffected by the conformation of the rest of the chain. For the $n = 12$ and $n = 16$ compounds, this region of the infrared spectrum is displayed in Figure 10, for different temperatures.

As the temperature is raised, we find peaks at 1341 cm^{-1} appearing that correspond to end-gauche defects and at 1364 cm^{-1} peaks appearing that correspond to kink defects. Double gauche defects, which would manifest at 1354 cm^{-1} are not seen. The nature of the observed defects (kinks and end-gauche) are typical of a system of densely packed (in the plane of the lipid layer) organic chains—the dense packing preventing those defects that require large volumes, such as double gauche, from making an appearance. The intensities of the individual components were obtained by spectral decomposition as a sum of Lorentzians after a suitable spline-fitted background subtraction.³² In Figure 11 are plots of the intensity ratio I_{1341}/I_{1377} and I_{1366}/I_{1377} for the $n = 12, 16$, and 18 compounds. The I_{1341}/I_{1377} ratio is characteristic of end-gauche sequences whereas the

I_{1366}/I_{1377} ratio to the concentration of kinks (g–t–g). The concentration of both the defects show a steady increase with temperature and appear to saturate above T_m . For all three compounds there were variations in the calculated intensity ratios for different batches; this may, in part, have been a consequence of the spectral decomposition and background subtraction procedures. The temperature variations were, however, identical.

The spectroscopic evidence so far suggests that the melting transition corresponds to a conformational disordering of the alkyl chains with the development of a large number of end-gauche and kink defects in the hydrocarbon chains. What then characterizes the premelting transition? We already know three things about this transition: (i) The c spacing actually decreases at this transition. (ii) The enthalpy change at this transition seems to be independent of the alkyl chain length. (iii) The transition does not have a simple signature in the C–H stretch or wagging region of the vibrational spectra, unlike the melting transition. The evidence, therefore, points to changes in the disposition of the ammonium headgroups across the premelting transition.

We have examined the N–H stretching region of the infrared spectrum of the three compounds as a function of temperature. The data are presented in Figure 12. At room temperature the spectra of all three compounds show three bands in the N–H stretching region, a broad band at 3020 cm^{-1} and two bands at 3110 and 3160 cm^{-1} . Above the T_1 , the premelting transition, the latter two bands broaden and collapse into a single broad band. This behavior is similar to the motional collapse of the methyl C–H asymmetric stretching modes reported in alkanes and other similar molecules.³³ The ammonium NH_3^+ group has three N–H stretching vibrations. A totally symmetric vibration (3020 cm^{-1}) and two asymmetric vibrations, which are degenerate for an ammonium group of at least C_3 symmetry. Symmetries lower than C_3 lift this degeneracy, and the asymmetric stretching modes appear split. The appearance of the bands at 3110 and 3160 cm^{-1} in the room-temperature spectra of $(C_nH_{2n+1}NH_3)_2PbI_4$, $n = 12, 16, 18$, indicates that the 3-fold symmetry of the

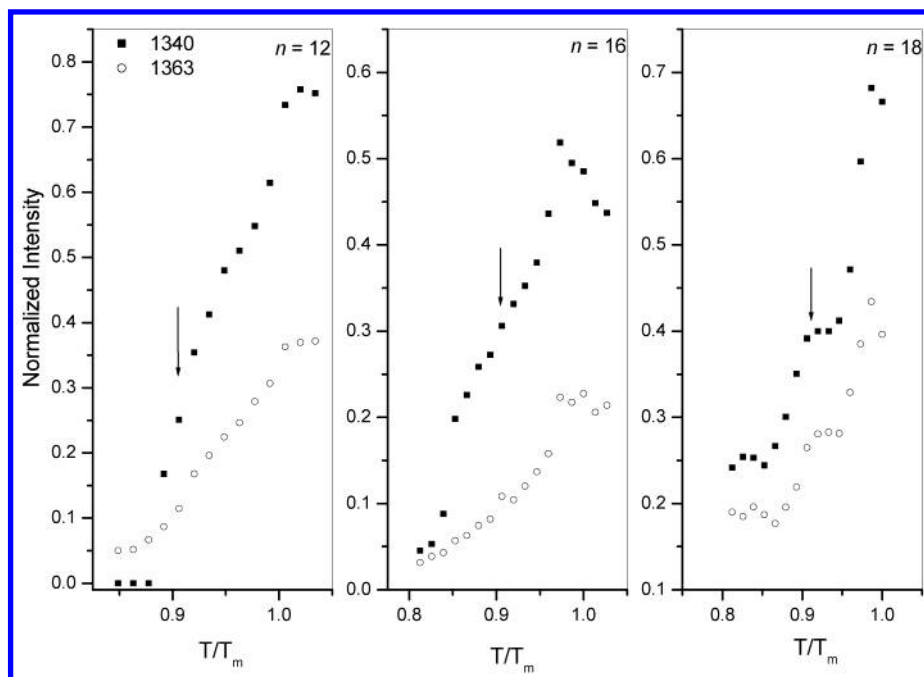


Figure 11. Variation in the intensity ratios of the end-gauche I_{1341}/I_{1377} and “kink” I_{1366}/I_{1377} peaks in $(C_nH_{2n+1}NH_3)_2PbI_4$, $n = 12, 16, 18$ as a function of reduced temperature. The temperature of the premelting transition is indicated by an arrow.

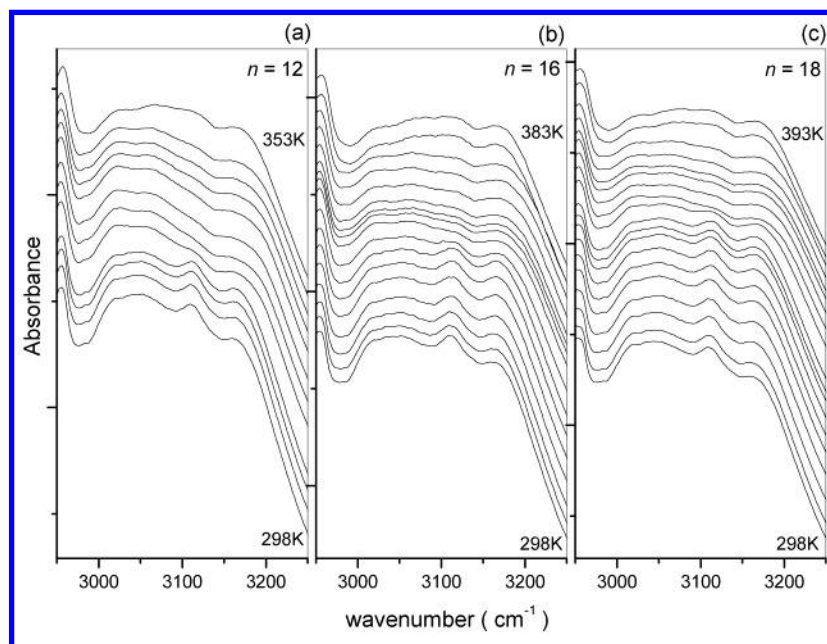


Figure 12. Infrared spectra of $(C_nH_{2n+1}NH_3)_2PbI_4$, (a) $n = 12$, (b) $n = 16$, and (c) $n = 18$, in the NH_3^+ “head” group region, showing the collapse of the NH_3^+ stretching modes above the premelting transition. The spectra were recorded at 5 K intervals.

$-NH_3^+$ group is broken. This is understandable because the $-NH_3^+$ group sits between the four I atoms in the PbI_4^{2-} square lattice—the problem of pegging a square hole with a triangular peg. The fact that the two peaks collapse to a single broad band above the premelting transition indicates that 3-fold symmetry is recovered. This suggests that the first transition is associated with the dynamic rotational disordering of the NH_3^+ groups. This would explain why the enthalpy change associated with the premelting transition is independent of the length of the methylene chain and why no significant change in conformational disorder is seen at T_1 neither in the infrared nor Raman spectra.

In many n -alkanes a solid–solid phase transition is observed at temperatures below the melting points. The lateral unit cell dimensions change, at the transition, so as to approach

hexagonal symmetry. It was proposed that molecules become effectively cylindrical as a result of executing rotation-like motion about their long axis.³⁴ Subsequently, this premelting or rotator phase transition has been observed in a number of alkyl chain assemblies including Langmuir–Blodgett (LB) films.³⁵ In the rotator phase molecules are envisioned to execute rotational jumps about their long axis while maintaining an all-trans extended geometry. Although premelting transition in $(C_nH_{2n+1}NH_3)_2PbI_4$ has features comparable with the rotator phase transition in n -alkanes and LB films, e.g., small ΔS associated with the transition, there are notable differences. Above the premelting transition (T_1) the C_3 symmetry of the NH_3^+ “head” group is recovered, indicating rotational disordering. This could arise either by rotational motion of the alkylammonium chain about its long axis similar to that in the rotator phase

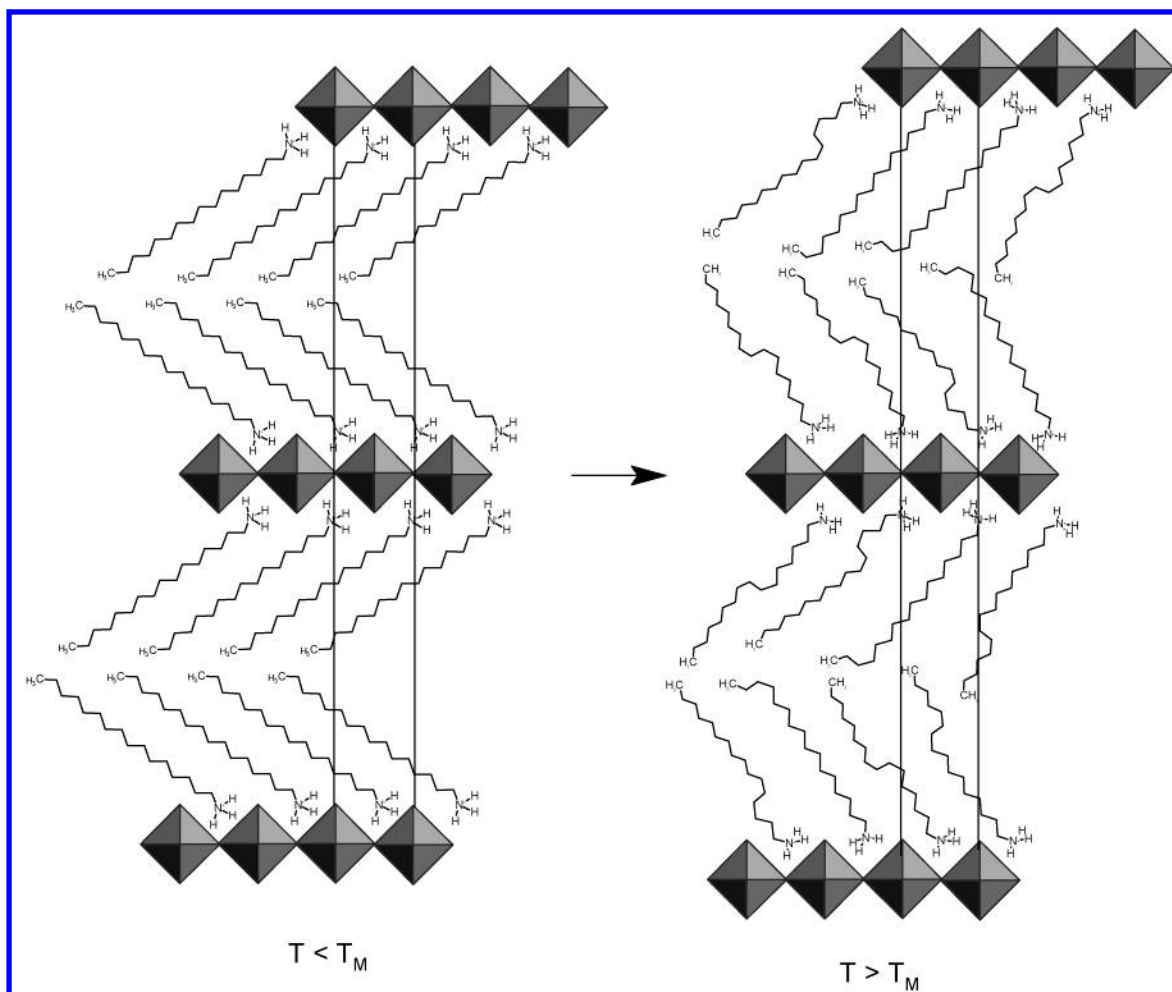


Figure 13. Schematic depiction of the melting transition in the $(C_nH_{2n+1}NH_3)_2PbI_4$ compounds. The structure on the left is the room temperature one in which the alkyl chains adopt an all-trans conformation with a well-defined tilt angle of 55° .^{18,19} The structure on the right is of the chains above the melting transition; chains are conformationally disordered and the tilt angle of individual chains are different.

of the alkanes or simply by a rotation of the NH_3 about the C–N bond of the “head” group of the alkylammonium chain. The former is the more likely scenario because both IR and Raman spectra indicate a steady rise in the concentration of gauche disorder between the premelting (T_i) and melting (T_m) transition. Consequently, not all alkyl chains are present in a rigid, fully extended, all-trans conformation expected of a rotator phase.

Conclusions

The layered inorganic–organic compounds $(C_nH_{2n+1}NH_3)_2PbI_4$, $n = 12, 16, 18$, comprise alkylammonium bilayers anchored to rigid perovskite-like PbI_2 sheets. At room temperature the methylene chains of the bilayer adopt an all-trans planar conformation with the molecular axis tilted at an angle of 55° with respect to the layer normal.¹⁸ With temperature these compounds exhibit two structural phase transitions associated with the organic moiety; a behavior similar to that of many lipid–bilayer systems. The first or premelting transition (T_i) exhibits considerable hysteresis, has an enthalpy change independent of the chain length (n), and is associated with a small contraction of the interlayer spacing. It is shown using the infrared spectroscopy that the C_3 symmetry of the NH_3^+ headgroup is recovered above this transition. The second or melting transition (T_m) is accompanied by a large dilation of the lattice along the interlayer axis. The enthalpy change on “melting” is proportional to the length of the alkylammonium

chain. The entropy change on “melting” per CH_2 in the chain, however, is roughly a constant. Both infrared and Raman spectroscopy indicate that the melting transition is associated with a large increase in gauche conformational disorder. The similarity of the Raman spectra of $(C_nH_{2n+1}NH_3)_2PbI_4$ compounds above T_m with those of n -alkanes in the melt provide direct evidence that although the main transition is strictly a solid–solid transition the methylene chains of the bilayer are liquidlike above this transition.

It is possible to reconstruct the sequence of events leading up to the main or “melting” transition in the $(C_nH_{2n+1}NH_3)_2PbI_4$, $n = 12, 16, 18$ compounds based on the evidence presented here. At room temperature the alkyl chains of the tilted bilayer are all-trans. The NH_3^+ headgroup that sits between the four I atoms of the square PbI_2 lattice is static, and consequently, its symmetry lowered from C_3 . With temperature a dynamic rotational disordering of the NH_3^+ group occurs at the premelting transition so that C_3 symmetry is recovered. Infrared (Figure 6) and Raman spectra (Figure 8) indicate that there is a steady buildup in the concentration of gauche conformers above the premelting transition leading to the melting of the alkyl chains. At T_m there is a sharp increase in conformational disorder. Because the alkylammonium chains are anchored, no lateral expansion of the chains is possible on melting, unlike in the case of the lipid bilayers or alkanes. The methylene chains in $(C_nH_{2n+1}NH_3)_2PbI_4$ are packed fairly densely. This may be gauged from the observation that double-gauche defects, which

require a larger volume, are prevented from making an appearance even at higher temperatures. Space or “free” volume, however, needs to be created to accommodate the increased concentration of gauche conformers at the melting transition. This may be achieved if the tilt angles of the individual alkylammonium chains no longer have identical values, i.e., a loss of tilt angle coherence on “melting”. Changes in tilt angle are possible because the “head” group is no longer frozen but rotationally disordered above the premelting transition. The loss of tilt coherence in turn would lead to an increase in the interlayer spacing, as shown in Figure 13. This is indeed observed in the X-ray diffraction of these compounds above the melting transition. A collective change from a uniquely defined tilt angle of the methylene chains to another as the cause of the lattice expansion at T_m may be ruled out because it would not create the additional free volume required to accommodate the increased concentration of gauche conformers in the melt.

Acknowledgment. S.B. thanks the CSIR, India, for a fellowship. R.S. is supported by the Department of Science and Technology, India.

References and Notes

- (1) Papavassiliou, G. C. *Prog. Solid. State. Chem.* **1997**, 25, 125.
- (2) Mitzi, D. B.; Field, C. A.; Harrison, W. T. A.; Guloy, A. M. *Nature* **1994**, 369, 467.
- (3) Papavassiliou, G. C.; Koutselas, I. B.; Terzis, A.; Whangbo, M. H. *Solid State Commun.* **1994**, 91, 695.
- (4) Ishihara, T.; Takahashi, J.; Goto, T. *Solid State Commun.* **1989**, 69, 933.
- (5) Ishihara, T.; Takahashi, J.; Goto, T. *Phys. Rev. B* **1990**, 42, 11099.
- (6) Hong, X.; Ishihara, T.; Nurmikko, A. V. *Phys. Rev. B* **1992**, 45, 6961.
- (7) Gennis, R. B. In *Biomembranes: Molecular Structure and Function*; Springer-Verlag: New York, 1989.
- (8) Jacobs, R. E.; Hudson, B. S.; Anderson, H. C. *Biochemistry* **1977**, 16, 4349.
- (9) Janiak, M. J.; Small, D. M.; Shipley, G. G. *Biochemistry* **1976**, 15, 4575.
- (10) Rand, R. P.; Chapman, D.; Larsson, K. *Biophys. J.* **1975**, 15, 1117.
- (11) Salerno, V.; Grieco, A.; Vacatello, M. *J. Phys. Chem.* **1976**, 22, 2444.
- (12) Blinc, R.; Burgar, M.; Lozar, B.; Seliger, J.; Slak, J.; Rutar, V.; Arend, H.; Kind, R. *J. Chem. Phys.* **1977**, 66, 278.
- (13) Kind, R.; Plesko, S.; Arend, R.; Blind, R.; Zeks, B.; Seliger, J.; Lozar, B.; Slak, J.; Levstik, C.; Filipic, C.; Zagar, V.; Lahajnar, G.; Milia, F.; Chapuis, G. *J. Chem. Phys.* **1979**, 71, 2118.
- (14) Needham, G. F.; Willett, R. D.; Franzen, H. F. *J. Phys. Chem.*, **1981**, 85, 3385.
- (15) Needham, G. F.; Willett, R. D.; Franzen, H. F. *J. Phys. Chem.* **1984**, 88, 674.
- (16) Casal, H. L.; Cameron, D. G.; Mantsch, H. H. *J. Phys. Chem.* **1985**, 85, 5557.
- (17) Almirante, C.; Minoni, G.; Zerbi, G. *J. Phys. Chem.* **1986**, 90, 852.
- (18) Venkataraman, N. V.; Bhagyalakshmi, S.; Vasudevan, S.; Ram Seshadri. *Phys. Chem. Chem. Phys.* **2002**, 4, 4553.
- (19) Venkataraman, N. V.; Barman, S.; Vasudevan, S.; Ram Seshadri. *Chem. Phys. Lett.* **2002**, 358, 139.
- (20) Traube, H.; Haynes, D. H. *Chem. Phys. Lipids* **1971**, 7, 324.
- (21) MacPhail, R. A.; Strauss, H. L.; Snyder, R. G.; Elliger, C. A. *J. Phys. Chem.* **1984**, 88, 334.
- (22) Snyder, R. G.; Strauss, H. L.; Elliger, C. A. *J. Phys. Chem.* **1982**, 86, 5145.
- (23) Snyder, R. G. *J. Mol. Spectrosc.* **1964**, 7, 116.
- (24) Snyder, R. G.; Liang, G. L.; Strauss, H. L.; Mendelsohn, R. *Biophys. J.* **1996**, 71, 3186.
- (25) Wallach, D. F. H.; Verma, S. P.; Fookson, J. *Biochim. Biophys. Acta* **1979**, 559, 153.
- (26) Snyder, R. G.; Hsu, S. L.; Krimm, S. *Spectrochim. Acta* **1978**, 34, 395.
- (27) Zerbi, G. In *Modern Polymer Spectroscopy*; Wiley-VCH: New York, 1999.
- (28) Zerbi, G.; Abbate, S. *Chem. Phys. Lett.* **1981**, 80, 455.
- (29) Zerbi, G.; Roncone, P.; Longhi, G.; Wunder, S. L. *J. Chem. Phys.* **1988**, 89, 166.
- (30) Snyder, R. G. *J. Chem. Phys.* **1967**, 47, 1316.
- (31) Maroncelli, M.; Qi, S. P.; Strauss, H. L.; Snyder, R. G. *J. Am. Chem. Soc.* **1982**, 104, 6237.
- (32) Venkatarama, N. V.; Vasudevan, S. *J. Phys. Chem. B* **2001**, 105, 1805.
- (33) MacPhail, R. A.; Snyder, R. G.; Strauss, H. L. *J. Chem. Phys.* **1982**, 77, 1118.
- (34) Ewen, B.; Strobl, G. R.; Richter, D. *Faraday Discuss. Chem. Soc.* **1980**, 69, 19.
- (35) Sirota, E. B. *Langmuir* **1997**, 13, 3849.